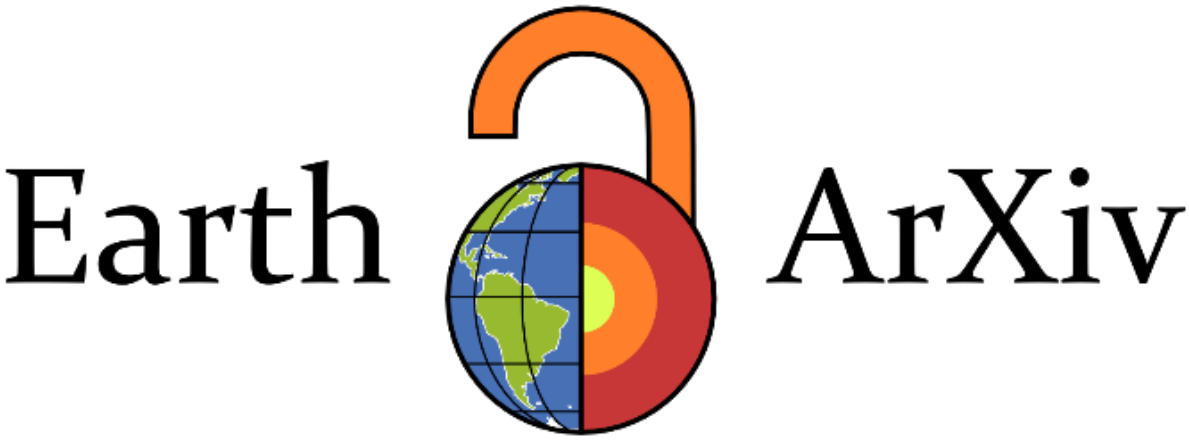

Mathematical Modeling of Coupled Heat and Mass Transfer with Phase Transitions in Heterogeneous Porous Soils: Mechanism of Soil Moisture Diffusivity Collapse during Freezing

Elena M. Avraham

Kuban State Agrarian University named after I.T. Trubilin, 13 Kalinina St., Krasnodar, 350044, Russia

Abstract. A mathematical model of coupled heat and mass transfer with water–ice–vapor phase transitions in heterogeneous porous soils is developed. The model comprises the Richards equation, the water vapor diffusion equation, and the heat transfer equation, coupled through a temperature-dependent hydraulic conductivity governed by the Kozeny–Carman relation and thermodynamic phase equilibrium described by the Clapeyron–van Genuchten framework. The study aims to identify the physical mechanism responsible for moisture transport suppression during soil freezing and to quantitatively characterize the sharp reduction in the soil moisture diffusion coefficient. An analytical expression for the soil moisture diffusion coefficient is derived, linking hydraulic conductivity to specific moisture capacity and governing the rate of moisture redistribution in the soil. It is shown that the behavior of the system can be described in compact dimensionless form controlled by a single governing parameter that separates two physically distinct limiting regimes of moisture transport degradation: a kinematic regime dominated by geometric pore blockage due to ice formation, and a thermodynamic regime governed by phase inertia associated with the latent heat of the phase transition. It is established that passage of the freezing front is accompanied by a sharp collapse of the soil moisture diffusion coefficient, caused by the simultaneous reduction of hydraulic conductivity and a manifold increase in the effective moisture capacity of the medium. The characteristic magnitude of the diffusivity reduction and the critical temperature corresponding to the transition between the kinematic and thermodynamic regimes of moisture transport suppression are determined. The results elucidate the physical mechanism of critical moisture transport suppression in freezing porous media and may be used in the development of thermo-hydrological models of frozen soils, prediction of seasonal soil freezing processes, and engineering assessment of soil foundation stability and infrastructure under cold-climate conditions.

Keywords: porous media; heat and mass transfer; water–ice phase transitions; moisture filtration; frozen soils; percolation; diffusion coefficient

Funding. This research received no external funding.

Conflict of interest. The authors declare no conflict of interest.

1. Introduction

Soil freezing and thawing processes play a key role in the formation of hydrological regimes, the stability of engineering structures, and the dynamics of the cryosphere under changing climate conditions. Below the freezing point, moisture and heat transport become a strongly coupled problem due to water–ice–vapor phase transitions accompanied by pore space redistribution, latent heat release and absorption, and a dramatic change in hydraulic conductivity. Experimental evidence shows that the filtration properties of soils may decrease by several orders of magnitude upon passage of the freezing front. However, the physical origin of this collapse remains debated: in existing models it is either prescribed through empirical impedance functions or emerges as a numerical effect within a fully coupled thermo-hydrodynamic formulation. The absence of a compact analytical description capable of separating the geometric and thermodynamic mechanisms of conductivity degradation substantially complicates the interpretation of simulation results and the construction of parametrically justified reduced models for permafrost hydrology and geotechnics.

The theoretical foundations of coupled heat and moisture transfer in porous media were established in the classical work [1], which proposed the first mechanistic description of thermally driven liquid and vapor fluxes. The Richards equation, widely used to describe moisture movement in unsaturated soils, was subsequently extended to freezing conditions and coupled with the heat transfer equation including latent heat. A major contribution to this formulation was made in [2], where a coupled thermo-hydraulic model was implemented in the HYDRUS software package, combining a modified Richards equation with heat transport and phase change descriptions. This formulation was successfully validated against laboratory experiments and currently forms the basis of most numerical studies of moisture and heat transfer in freezing soils.

A key element of thermo-hydrological models of frozen soils is the parameterization of the freezing curve relating temperature to liquid water content. Early approaches relied on empirical power-law dependencies; however, later work demonstrated that the freezing curve can be derived as a direct thermodynamic analogue of the soil water retention curve via Clapeyron equilibrium. This approach provides a consistent description of drying and freezing processes and has become the standard in modern land surface and permafrost hydrology models.

Significant uncertainty in existing models concerns the description of ice effects on hydraulic conductivity. The most common approach employs empirical ice impedance functions in which conductivity decreases exponentially with increasing ice content. In particular, [3] proposed a relation of the form $K_{\text{frozen}} = 10^{-\Omega\theta_i} K_{\text{thawed}}$, where Ω is an empirical parameter. More physically motivated formulations accounting for pore space geometry and excluded ice volume have also been proposed. Direct measurements of permeability in frozen soils have demonstrated hydraulic conductivity reductions of 2–3 orders of magnitude; however, the soil moisture diffusion coefficient, which simultaneously reflects conductivity and the storage term, has received little systematic analytical attention.

An additional complexity arises from the spatial heterogeneity of soils. Observations show that even at sub-zero temperatures, part of the pore space may remain hydraulically active, forming high-conductivity transport pathways. Such unfrozen channels and macropores can govern water flux distributions in partially frozen soils. Nevertheless, most existing models either assume homogeneous medium properties or account for heterogeneity only in a statistical sense, without explicit spatial description.

The objective of this study is to quantitatively investigate the mechanisms of hydraulic mobility degradation in heterogeneous soils during freezing and to identify the physical mechanism of soil moisture diffusivity collapse near the freezing front. To achieve this objective, the following tasks were formulated:

- To develop a fully coupled numerical model of heat and mass transfer in a heterogeneous porous medium describing the simultaneous transport of liquid water, water vapor, and heat with explicit treatment of the water–ice phase transition.
- To derive an analytical expression for the effective soil moisture diffusion coefficient in a freezing soil, accounting for two key mechanisms — geometric blockage of the pore space by ice and the increase of effective moisture capacity due to the latent heat of the phase transition — and to cast it in compact dimensionless form.
- To numerically investigate the evolution of the soil moisture diffusion coefficient upon passage of the freezing front and to quantitatively characterize the magnitude of its reduction.
- To separate the contributions of two physical suppression mechanisms — reduction of hydraulic conductivity due to pore blockage by ice and increase of effective moisture capacity due to the latent heat of the phase transition.
- To investigate the effect of spatial heterogeneity of soil parameters on the structure of moisture transport and to establish the connection between loss of liquid-phase connectivity in the pore space and the percolation threshold.
- To determine the dimensionless governing parameter characterizing the competition between geometric and thermodynamic suppression mechanisms and to establish the conditions for transition between the corresponding regimes.

2. Problem Formulation

The computational domain is modeled as a two-dimensional vertical cross-section of the soil profile:

$$\Omega = [0,\, L]^2$$

The vertical axis z is directed upward: $z = 0$ corresponds to the lower boundary of the domain and $z = L$ to the soil surface. Heat and mass transfer with water–ice–vapor phase transitions in a

heterogeneous porous soil medium is described by a system of three coupled nonlinear partial differential equations in the unknowns: matric potential $h(\mathbf{x},t)$, temperature $T(\mathbf{x},t)$, and water vapor density $\rho_v(\mathbf{x},t)$.

The conservation of water mass (liquid and ice phases) is written in the canonical form of the Richards equation [4, 5]:

$$\frac{\partial}{\partial t}\left[\theta(h) + \frac{\rho_i}{\rho_w}\theta_{\text{ice}}(h,T)\right] + \nabla \cdot \mathbf{q}_w = \frac{S_v}{\rho_w} - S_{\text{root}} \tag{1}$$

where $\theta(h)$ is the volumetric liquid water content, $\theta_{\text{ice}}(h,T)$ is the volumetric ice fraction, and ρ_i, ρ_w are the densities of ice and water, respectively. The term S_v describes the volumetric rate of the liquid–vapor phase transition (evaporation/condensation in the pore space), and S_{root} is the volumetric sink due to root water uptake. Phase distribution of water is described following [6, 7]. It is assumed that the total water content θ_w is conserved, and redistribution between liquid and ice phases is governed by the Clapeyron equation relating matric potential $h(\mathbf{x},t)$ and temperature $T(\mathbf{x},t)$ at the freezing front:

$$h(T) = \frac{L_f}{g}\ln\frac{T}{T_f}, \qquad T < T_f$$

where L_f is the specific latent heat of fusion, g is gravitational acceleration, and T_f is the phase transition temperature. Liquid water content is expressed through the water retention curve:

$$\theta_l(T) = \theta_{\text{VG}}(h(T))$$

and the volumetric ice fraction is determined as the difference between total and liquid water contents:

$$\theta_{\text{ice}}(T) = \theta_w - \theta_l(T) = \theta_w - \theta_{\text{VG}}(h(T))$$

Liquid water flux is given by Darcy's law [8]:

$$\mathbf{q}_w = -K(h,T)\,\nabla(h+z)$$

where $K(h,T)$ is the effective hydraulic conductivity depending on matric potential and temperature (through ice-induced pore blockage), and $h+z$ is the pressure head. The volumetric liquid water content is described by the van Genuchten model [9]:

$$\theta(h) = \begin{cases} \theta_r + \dfrac{\theta_s - \theta_r}{\left[1 + (\alpha_{\text{VG}}|h|)^{n_{\text{VG}}}\right]^{m_{\text{VG}}}}, & h < 0 \\[2ex] \theta_s, & h \geq 0 \end{cases}$$

where $m_{\text{VG}} = 1 - 1/n_{\text{VG}}$, $\theta_r(\mathbf{x})$ is residual water content, $\theta_s(\mathbf{x})$ is saturated water content, $\alpha_{\text{VG}}(\mathbf{x})$ is the capillary pressure scaling parameter, and $n_{\text{VG}}(\mathbf{x})$ is the dimensionless shape

parameter of the retention curve. Relative hydraulic conductivity is described by the Mualem–van Genuchten model [10]:

$$K_r(h) = S_e^{1/2}\Big[1 - \Big(1 - S_e^{1/m_{\mathrm{VG}}}\Big)^{m_{\mathrm{VG}}}\Big]^2, \qquad S_e = \frac{\theta(h) - \theta_r}{\theta_s - \theta_r}$$

The ice fraction in the pore space is derived from the soil freezing curve [11]:

$$f_{\mathrm{ice}}(T, \mathbf{x}) = \frac{\theta(h) - \theta_l(T, \mathbf{x})}{\theta_s(\mathbf{x})}$$

$$\theta_l(T, \mathbf{x}) = \begin{cases} \theta_r + \dfrac{\theta_s - \theta_r}{\Big[1 + \Big(\alpha_{\mathrm{VG}} \dfrac{L_f}{g T_f} |T - T_f|\Big)^{n_{\mathrm{VG}}}\Big]^{m_{\mathrm{VG}}}}, & T < T_f \\[2ex] \theta(h), & T \geq T_f \end{cases}$$

Reduction of hydraulic conductivity upon freezing is modeled by the cubic Kozeny–Carman law [12, 13]:

$$f_K(T) = \big(1 - f_{\mathrm{ice}}(T)\big)^3$$

Total hydraulic conductivity is written as:

$$K(h, T) = \max\big(K_s(\mathbf{x}) \cdot K_r(h) \cdot f_K(T),\; K_{\min}\big)$$

where $K_s(\mathbf{x})$ is the spatially variable saturated conductivity.

Heat transfer in the soil is described by an equation with effective heat capacity accounting for the phase transition [14]:

$$\rho C_{\mathrm{eff}}(T, \theta) \frac{\partial T}{\partial t} - \nabla \cdot \big[k_{\mathrm{eff}}(T, \theta) \nabla T\big] + \rho_w c_w\, \mathbf{q}_w \cdot \nabla T + \nabla \cdot (L_v \mathbf{q}_v) = Q_r \tag{2}$$

where the first term describes heat accumulation in the medium, the second thermal conductivity, the third advective heat transport by the liquid phase, and the fourth latent heat transport associated with water vapor diffusion. The effective volumetric heat capacity is:

$$\rho C_{\mathrm{eff}}(T, \theta) = C_{\mathrm{vol}}(T, \theta) + \rho_w L_f\, \theta(h) \left| \frac{\partial f_{\mathrm{ice}}}{\partial T} \right|$$

where the volumetric heat capacity of the soil–water mixture is:

$$C_{\mathrm{vol}}(T, \theta) = (1 - \theta_s)\rho_s c_s + \theta_l \rho_w c_w + \theta_{\mathrm{ice}} \rho_i c_i + (\theta_s - \theta_l - \theta_{\mathrm{ice}})\rho_a c_a$$

The temperature-dependent volumetric heat capacity of moist soil is given by:

$$\rho_{\mathrm{wet}}(T) = \rho_{\mathrm{wet},0}\big(1 + \beta_T (T - T_0)\big)$$

Effective thermal conductivity of the soil is given by:

$$k_{\mathrm{eff}}(T,\theta) = k_{\mathrm{dry}} + \theta\Big(k_{\mathrm{wet},0}\, e^{\gamma (T - T_0)} - k_{\mathrm{dry}}\Big)$$

where k_{dry} is the thermal conductivity of dry soil, $k_{\mathrm{wet},0}$ is the conductivity of fully water-saturated soil at temperature T_0, and γ is the temperature coefficient.

Water vapor transport in the pore space is described in conservative form with respect to gas-filled porosity:

$$\frac{\partial (\theta_g \rho_v)}{\partial t} + \nabla \cdot \mathbf{q}_v = S_v \tag{3}$$

where the vapor flux is given by Fick's law: $\mathbf{q}_v = -D(T,\theta_g)\,\nabla \rho_v$. Gas-filled porosity θ_g is defined as the volumetric fraction of the gaseous phase in the total soil volume:

$$\theta_g = \theta_s - \theta(h)\,(1 - f_{\mathrm{ice}})\, f_{\mathrm{ice}} = \theta_s - \theta(h)$$

The effective vapor diffusion coefficient in the gas phase is calculated using the Millington–Quirk model with the Cass correction factor [15]:

$$D_v(T,\theta_g) = D_v^0 \Big(\frac{T}{273.15}\Big)^{1.75} \cdot \frac{\theta_g^{10/3}}{\theta_s^2} \cdot \eta(\theta_g,\theta_s)$$

where the enhancement factor η is [16]:

$$\eta = 9.5 + 3.0\frac{\theta_g}{\theta_s} - 8.5\exp\!\Big[-\Big(1 + \frac{2.6}{\sqrt{\theta_s}}\Big)\frac{\theta_g}{\theta_s}\Big], \qquad \eta \geq 1$$

and D_v^0 is the molecular diffusivity of water vapor in air at 273.15 K. The volumetric rate of the liquid–vapor phase transition in the pore space is:

$$S_v = k_{\mathrm{evap}}\, \theta_g \big(\rho_v^{\mathrm{sat}}(T) - \rho_v\big)$$

Saturated vapor density is computed using the Tetens formula:

$$\rho_v^{\mathrm{sat}}(T) = \begin{cases} 4.85\times 10^{-3}\exp\!\Big(\dfrac{17.27(T-273.15)}{T-35.85}\Big), & T \geq T_f \\[2mm] 4.85\times 10^{-3}\exp\!\Big(\dfrac{21.87(T-273.15)}{T-7.65}\Big), & T \leq T_f \end{cases}$$

3. Initial and Boundary Conditions

Initial distributions of the unknown variables are prescribed as linear profiles along the vertical coordinate z. The initial matric potential is:

$$h(x,z,0) = -2.0 - 0.5\Big(1 - \frac{z}{L}\Big)$$

corresponding to a near-hydrostatic pressure distribution with a small vertical gradient. The initial temperature field is prescribed as a linear function:

$$T(x, z, 0) = 268.0 + \frac{285.0 - 268.0}{L}\, z$$

The initial vapor density equals the saturated value at the local temperature:

$$\rho_v(x, z, 0) = 4.85 \times 10^{-3} \exp\!\left(\frac{17.27\big(T_0(z) - 273.15\big)}{T_0(z) - 35.85} \right)$$

where $T_0(z) = T(x, z, 0)$ is the initial temperature profile.

At the lower boundary Γ_3, temperature is fixed: $T|_{\Gamma_3} = 268.0$ K. A free drainage condition is applied for the moisture flux: $\mathbf{q}_w \cdot \mathbf{n} = K(h, T)\, \nabla H \cdot \mathbf{n}$. At the upper boundary Γ_4 (soil surface), the thermal regime is described by a Robin condition:

$$\left(-k_{\text{eff}} \frac{\partial T}{\partial n} \right)\Big|_{\Gamma_4} = h_c (T - T_{\text{atm}}) - \alpha_s I_{\text{sun}}(t) - \rho_w c_w q_{\text{irr}} (T_w - T) - L_v\, \mathbf{q}_v \cdot \mathbf{n}$$

where h_c is the convective heat transfer coefficient, T_{atm} is the air temperature, α_s is the solar radiation absorption coefficient, $I_{\text{sun}}(t)$ is the diurnal insolation function, and $q_{\text{irr}}(t)$ is the prescribed surface irrigation mass flux. Vapor exchange with the atmosphere at the upper boundary is described by a Robin condition:

$$\left(-D_v \frac{\partial \rho_v}{\partial n} + k_{\text{atm}} (\rho_v - \rho_v^{\text{atm}}) \right)\Big|_{\Gamma_4} = 0$$

4. Numerical Implementation

The coupled system of equations (1), (2), and (3) is solved within a variational formulation using the finite element method. Spatial discretization is performed in the mixed functional space $W_h = P_1 \times P_1 \times P_1$, where P_1 denotes continuous piecewise-linear Lagrange elements of first order. The unknown fields of matric potential h, temperature T, and vapor density ρ_v are approximated by functions from W_h. The weak form of the system is obtained by multiplying the governing equations by corresponding test functions $(v_h, v_T, v_{\rho_v}) \in W_h$ and integrating by parts. Time discretization is performed using a first-order implicit Euler scheme with time step Δt over a simulation interval comprising N time steps. Time derivatives are approximated as:

$$\frac{u^{n+1} - u^n}{\Delta t} \approx \frac{\partial u}{\partial t}$$

At each time step, the resulting nonlinear system of algebraic equations is solved by the Newton–Raphson method. The Jacobian of the variational form is computed by automatic

differentiation, $J = dF/dw$, ensuring consistency of the linear approximation with the nonlinear formulation and stability of the iterative process.

5. Model Verification

The numerical scheme was verified in three stages: (1) accuracy of the Richards equation solver against the analytical Philip solution; (2) validation of the thermal module against the classical Carslaw–Jaeger solution; (3) validation of the full coupled model against measured temperature profiles in permafrost soils of Yakutsk from the NSIDC G02189 dataset. This multi-level verification strategy is consistent with the methodology accepted in the literature for thermo-hydrological model testing and allows sequential separation of numerical errors from features of the physical problem formulation.

Richards equation verification. Two tests were performed to separate numerical errors from physical model features. In the first test, a linear form of the Richards equation with constant hydraulic capacity $C = d\theta/dh = \text{const}$ was used, reducing the problem to a diffusion equation with Philip's analytical infiltration solution [1]. The numerical solution on a 40×40 grid at $t = 1000$ s reproduces the analytical moisture profile with $R^2 = 0.9998$, $\mathrm{RMSE} = 0.0005$, and $\mathrm{MAE} \approx 0.0004$, consistent with benchmark Richards equation solver verifications reported in [17, 18]. In the second test, the nonlinear van Genuchten retention model was used with parameters $\alpha = 0.7$, $n = 1.6$, $\theta_r = 0.15$, $\theta_s = 0.45$. The numerical solution correctly reproduces the characteristic infiltration front shape observed in real soils, with $\mathrm{MAE} = 0.005$, $\mathrm{RMSE} = 0.012$, and $R^2 = 0.871$.

Heat transfer equation verification. The heat equation was verified against the Carslaw–Jaeger analytical solution for a semi-infinite medium with initial temperature $T_0 = 273$ K and a step surface heating to $T_s = 373$ K [19]. This solution is a classical test for heat transport models and is widely used in the verification of frozen soil numerical schemes. Simulations were performed with soil parameters $\rho = 1500$ kg/m³, $c_p = 800$ J/(kg·K), $k = 1.5$ W/(m·K), giving thermal diffusivity $\alpha = 1.25 \times 10^{-6}$ m²/s, in a domain of depth 0.5 m with a time step of 10 s. The mean RMSE over the full simulation period was 0.026 K; the maximum error at the initial moment reached 0.063 K and decreased monotonically to 0.011 K at final time, confirming the absence of error accumulation. The achieved accuracy is substantially better than the 1 K threshold accepted in the cryosphere modeling literature.

Validation against field data (Yakutsk). The full coupled model was validated against measured temperature profiles in permafrost soils of Yakutsk (1971) published in the NSIDC G02189 dataset [20]. This dataset is widely used for evaluation of thermo-hydrological permafrost models. Simulations were conducted for a domain of depth 3.5 m with a 1-hour time step over a 2-year period, with the first year used as initialization. Soil parameters were chosen in accordance with typical values for Central Yakutia silty loam. A Robin boundary condition with seasonal air

temperature from NSIDC was applied at the upper boundary, while the lower boundary temperature was fixed at $T_{\text{bot}} = -5$°C. An effective heat transfer coefficient $h_c = 0.5$ W/(m²·K) accounted for the insulating effect of approximately 50 cm of snow cover. Comparison of modeled and observed temperature profiles shows excellent agreement. For depths 0.40–3.20 m, RMSE is 0.09 K in January and 0.07 K in July, with $R^2 = 0.9998$. These values are comparable to or better than state-of-the-art permafrost models: CLM4.5 (RMSE 0.3–1.2 K) [21], CryoGrid (RMSE 0.5–0.8 K) [22], and JSBACH (RMSE < 0.5 K) [23].

Mass and energy balance diagnostics. Correctness of the numerical implementation was additionally verified by monitoring mass balances of water (liquid, ice, and vapor phases) and energy at each time step. The vapor mass balance closed to machine precision: the finite element change in vapor mass was -0.042105 mg, while the sum of evaporation sources and boundary fluxes gave -0.042108 mg, with an absolute error of 3×10^{-6} mg. Full consistency was achieved for the combined liquid and ice water mass balance: the change in volumetric water content computed from the field $\theta_l + (\rho_i/\rho_w)\theta_i$ amounted to 2.2×10^{-9} m³ and coincided exactly with the difference between current and initial water mass in the domain. The total contribution of evaporation, condensation, root uptake, and drainage gave -9.8651×10^{-8} m³, with a discrepancy between computed and predicted mass change of 5×10^{-15} m³ (relative error below 10^{-4}%). The change in internal energy of the system computed directly from the temperature field agreed with the flux-balance prediction to 3.6×10^{-3} J, corresponding to a relative error of order 10^{-4}%. Additional physical checks confirmed that all computed fields remained within admissible ranges and entropy production remained positive, confirming thermodynamic consistency of the numerical scheme. The performed tests thus demonstrate strict conservation of the model with respect to water mass (in all phases) and energy, and correct implementation of source terms and boundary fluxes. This confirms that the effects identified below are physical consequences of the model rather than numerical artifacts.

6. Collapse of the Soil Moisture Diffusion Coefficient during Freezing

Analysis of simulation results reveals a sharp change in the soil moisture diffusion coefficient upon passage of the freezing front. In the thawed zone, the mean value of the soil moisture diffusion coefficient is $D_{\text{eff}}(T > 0^\circ\text{C}) \approx 3.7 \times 10^{-6}$ m²/s, while in the frozen zone it decreases to $D_{\text{eff}}(T < 0^\circ\text{C}) \approx 3.6 \times 10^{-10}$ m²/s. Thus, freezing leads to a reduction of the soil moisture diffusion coefficient by more than four orders of magnitude.

Analysis of individual mechanism contributions shows that this effect results from the simultaneous action of two processes. First, ice formation leads to blockage of the pore space and reduces hydraulic conductivity by a factor of approximately 158. Second, near the phase transition temperature, the effective capacity of the system increases sharply due to the latent heat of freezing.

In the transition zone, the ratio of the latent and hydraulic capacity components reaches $C_{\text{latent}}/C_{\text{hyd}} \approx 260$, which further suppresses the rate of moisture redistribution.

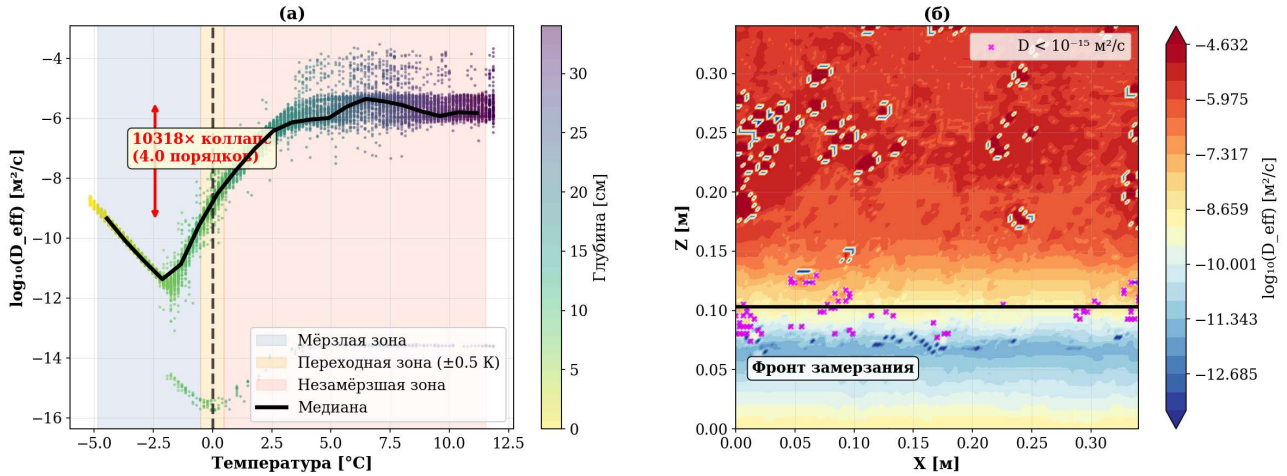

Figure 1 — *Collapse of the soil moisture diffusion coefficient during freezing of heterogeneous soil. Dependence of* $\log_{10}(D_{\text{eff}})$ *on temperature (a): points are colored by depth, black line is the median curve over temperature bins; frozen (blue), transitional (orange), and thawed (red) zones are indicated. The arrow shows the magnitude of the diffusivity collapse upon passage of the freezing front. Spatial distribution of* $\log_{10}(D_{\text{eff}})$ *in the computational domain (b); the black isoline corresponds to the freezing front* ($T = 0°C$).

The obtained results are consistent with a percolation theory interpretation. Fitting the dependence of the soil moisture diffusion coefficient on liquid fraction yielded power-law behavior of the form $D_{\text{eff}} = D_0(f_l - f_c)^{\mu}$, where $f_c \approx 0.3$ corresponds to the percolation threshold and the critical exponent $\mu \approx 1.3$ agrees with theoretical values for two-dimensional random media. This indicates that the collapse of the soil moisture diffusion coefficient is associated with loss of liquid-phase connectivity in the pore space as the ice fraction grows.

Additional analysis showed that the effect persists when physically realistic values of minimum hydraulic conductivity are used. Even with $K_{\min} = 10^{-12}$ m/s, the reduction of the soil moisture diffusion coefficient remains more than four orders of magnitude. This confirms that the observed collapse is a consequence of the physics of the freezing process and not a numerical artifact.

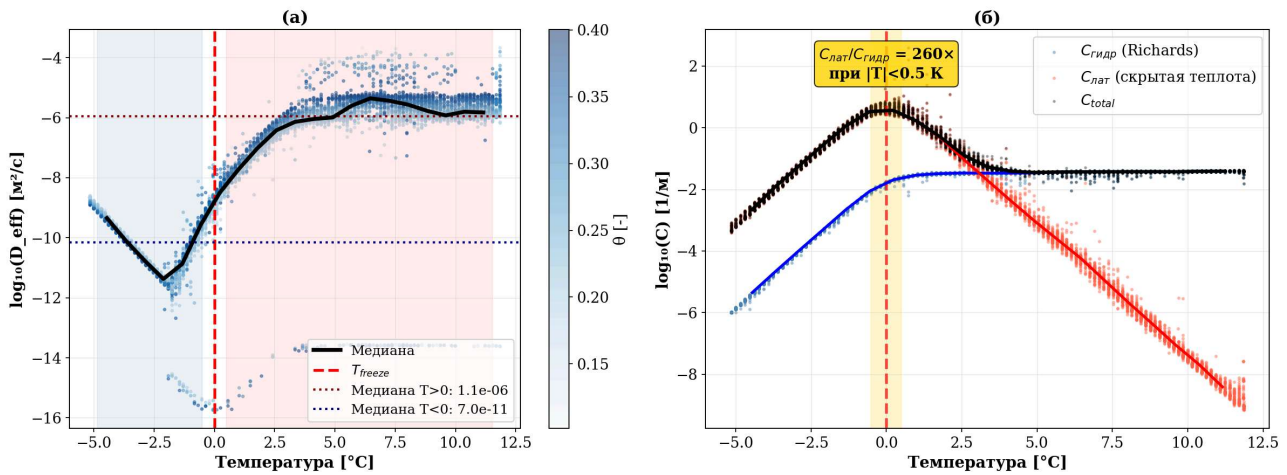

Figure 2 — *Mechanism of soil moisture diffusivity collapse: role of ice-induced pore blockage and latent heat buffering. Soil moisture diffusion coefficient (a) $D_{\text{eff}} = K_{\text{frz}}/C_{\text{total}}$ as a function of temperature; points are colored by volumetric moisture content θ, dashed lines show median values in the thawed and frozen zones. Components of the moisture retention coefficient (b): hydraulic capacity C_{hyd}, latent heat capacity C_{lat}, and total capacity C_{total}. The gold band marks the transition zone where the ratio $C_{\text{lat}}/C_{\text{hyd}}$ reaches its maximum.*

Thus, the simulation results demonstrate the existence of a critical moisture transport regime near the freezing front in which the joint action of geometric pore blockage and the increase of latent heat capacity leads to sharp suppression of the soil moisture diffusion coefficient.

7. Analytical Formula for Soil Moisture Diffusivity in Freezing Heterogeneous Soil

The soil moisture diffusion coefficient of a freezing porous medium, accounting for ice-induced pore blockage and moisture transport suppression by the latent heat of the phase transition, is given by:

$$\frac{D_{\text{eff}}(\mathbf{x},T)}{D_0(\mathbf{x})} = \frac{\left[1 - f_{\text{ice}}(T)\right]^3}{1 + B(\mathbf{x},T)\left|\dfrac{\partial f_{\text{ice}}}{\partial T}\right|} \tag{4}$$

where $D_{\text{eff}}(\mathbf{x},T)$ is the soil moisture diffusion coefficient of the freezing soil, $D_0(\mathbf{x})$ is the soil moisture diffusion coefficient in the absence of ice ($T \geq T_0$), and $f_{\text{ice}}(T)$ is the pore ice fraction. The dimensionless coupling parameter between hydraulics and thermophysics is:

$$B(\mathbf{x},T) = \frac{\rho_w L_f\, \theta_s(\mathbf{x},T)}{C_V(\mathbf{x},T)} \tag{5}$$

where ρ_w is water density, L_f is the specific latent heat of fusion, θ_s is the volumetric water content at saturation, and C_V is the volumetric heat capacity defined as:

$$C_V(\mathbf{x},T) = (1-\phi)\rho_s c_s + \theta_l \rho_w c_w + \theta_i \rho_i c_i$$

where ϕ is porosity, ρ_s, ρ_w, ρ_i are densities of the solid phase, water, and ice, c_s, c_w, c_i are their specific heat capacities, θ_l is the volumetric liquid water fraction, and θ_i is the volumetric ice fraction. Liquid water content is given by the modified van Genuchten relation:

$$\theta_l(\mathbf{x},T) = \theta_r + (\theta_s - \theta_r)\left[1 + \left(\alpha_{\text{frz}}|h^*(T)|\right)^n\right]^{-m}, \qquad T \leq T_0$$

where θ_r is residual moisture content, α_{frz}, n, m are empirical parameters, and T_0 is the phase transition temperature. The volumetric ice fraction is derived from the Clausius–Clapeyron equation and the van Genuchten framework:

$$f_{\text{ice}}(T) = \max\!\left(0,\; 1 - \frac{\theta_l(T)}{\theta_s}\right), \qquad h^*(T) = \frac{L_f(T - T_0)}{g\,T_0}$$

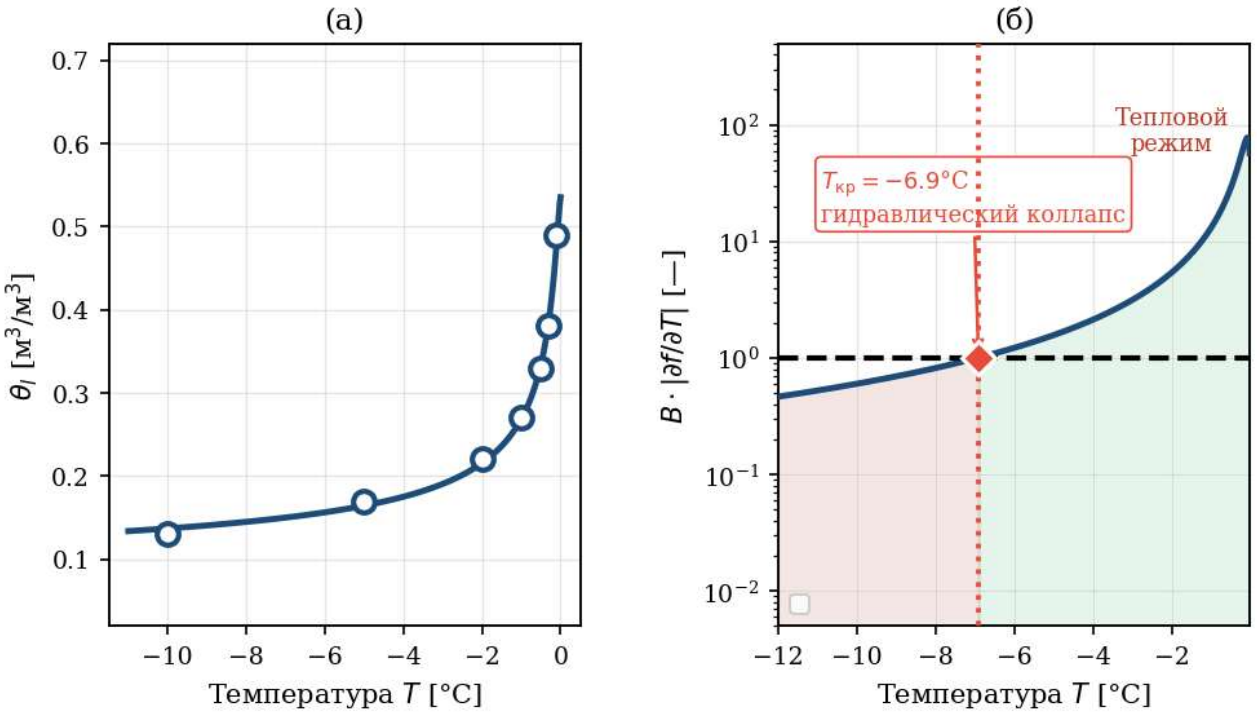

Figure 3 — *Verification of the freezing curve and hydraulic collapse criterion for silty loam. (a) Volumetric liquid water content θ_l as a function of temperature: solid line — van Genuchten model with fitted parameters, circles — experimental data [4]. (b) Temperature dependence of the dimensionless parameter $\Pi \equiv B(\mathbf{x}, T)|\partial f_{\text{ice}}/\partial T|$ determining the regime of filtration degradation: the dashed horizontal line corresponds to the criterion $\Pi = 1$, the red point — critical temperature T_{cr} at which the regime transition occurs. Red zone — thermodynamic regime ($\Pi > 1$), in which phase inertia of the latent heat suppresses hydraulic transport. Green zone — kinematic regime ($\Pi < 1$), in which filtration degradation is governed by geometric pore blockage by ice.*

The derived expression for the relative soil moisture diffusion coefficient (4) admits a natural asymptotic interpretation through the dimensionless parameter:

$$\Pi \equiv B(\mathbf{x}, T) \left| \frac{\partial f_{\text{ice}}}{\partial T} \right| \tag{6}$$

which fully determines the regime of hydraulic mobility degradation during freezing. In the limit $\Pi \ll 1$, the denominator approaches unity and the diffusion coefficient is governed solely by the geometric pore-blocking factor: $D_{\text{eff}}/D_0 \approx (1-f)^3$. This is the kinematic regime, realized at deep sub-zero temperatures when the freezing curve reaches a plateau and $|\partial f/\partial T| \to 0$: the phase transition is practically complete and filtration suppression is controlled only by the reduction of effective porosity. In the opposite limit $\Pi \gg 1$, phase inertia dominates: $D_{\text{eff}}/D_0 \approx [(1-f)^3 C_V]/[\rho_w L_f |\partial\theta_l/\partial T|]$, corresponding to the thermodynamic control regime — any hydraulic perturbation drives primarily phase redistribution rather than liquid transport, since latent heat absorbs the hydraulic storage capacity of the system. Near the freezing point, where via Clapeyron equilibrium $h^*(T) \propto |T|$, the van Genuchten model gives $|\partial\theta_l/\partial T| \propto |T|^{n-1}$, and consequently $D_{\text{eff}}/D_0 \to 0$ as $|T|^{n-1}$. The collapse rate is thus governed by the shape parameter n,

linking the character of conductivity degradation directly to soil texture. The boundary between regimes is defined by the condition $\Pi = 1$, which yields an implicit analytical equation for the critical temperature T_{cr} depending on the pore structure parameters and thermophysical properties of the medium. The formula thereby identifies two fundamentally distinct mechanisms of filtration suppression — geometric pore blockage and thermodynamic phase inertia — and introduces an explicit criterion for their competition, which gives the reduced model independent analytical value.

8. Conclusions

A mathematical model of coupled heat and mass transfer with water–ice–vapor phase transitions in heterogeneous porous soils has been developed and a numerical analysis of moisture transport processes under freezing conditions has been performed. The model is based on the Richards equation, water vapor diffusion equation, and heat transfer equation, coupled through a temperature-dependent hydraulic conductivity and thermodynamic phase equilibrium.

It is shown that passage of the freezing front is accompanied by a sharp reduction in the soil moisture diffusion coefficient. In the thawed zone, characteristic values of the diffusion coefficient are $D_{\text{eff}} \approx 3.7 \times 10^{-6}$ m²/s, while in the frozen zone they decrease to $D_{\text{eff}} \approx 3.6 \times 10^{-10}$ m²/s. Thus, freezing leads to a collapse of the soil moisture diffusion coefficient by more than four orders of magnitude, corresponding to critical suppression of moisture transport near the freezing front.

Analysis of the governing equations reveals that this effect results from the joint action of two physical mechanisms. The first is geometric blockage of the pore space by ice, which reduces hydraulic conductivity of the medium. The second is the sharp increase in effective moisture capacity of the system due to the latent heat of the phase transition. Near the freezing temperature, the ratio of latent and hydraulic capacity components reaches $C_{\text{latent}}/C_{\text{hyd}} \approx 260$, which substantially retards moisture redistribution.

Numerical analysis of a spatially heterogeneous medium demonstrates that transport capacity degradation has a percolation character. The dependence of the soil moisture diffusion coefficient on liquid fraction follows power-law behavior $D_{\text{eff}} = D_0(f_l - f_c)^{\mu}$, where $f_c \approx 0.3$ corresponds to the percolation threshold and the critical exponent $\mu \approx 1.3$ is close to theoretical values for random porous media. This indicates that the diffusivity collapse is associated with loss of liquid-phase connectivity in the pore space as the ice fraction grows. Calculations confirmed the robustness of the observed effect across physically justified ranges of minimum hydraulic conductivity, ruling out a numerical origin and confirming the physical nature of the diffusivity collapse.

The principal theoretical result of this work is the derivation of analytical expression (4) for the relative soil moisture diffusion coefficient in a freezing heterogeneous soil, simultaneously accounting for geometric pore blockage by ice and moisture transport suppression through the

increase of effective moisture capacity driven by the latent heat of the phase transition. The derived formula yields a compact dimensionless representation and introduces the governing parameter Π determining the regime of moisture transport suppression during freezing. It is shown that for $\Pi \ll 1$ the kinematic regime prevails, in which transport suppression is governed primarily by the geometric reduction of effective porosity, while for $\Pi \gg 1$ the thermodynamic regime dominates, associated with phase inertia of the system and increase of effective moisture capacity. The derived analytical expression thus establishes a quantitative criterion for the relative contribution of geometric and thermodynamic suppression mechanisms.

The scientific novelty of the work is as follows:

- A collapse of the soil moisture diffusion coefficient upon passage of the freezing front in heterogeneous porous soils has been numerically identified and quantitatively characterized, leading to a reduction in moisture transport intensity by more than four orders of magnitude.
- It is shown that degradation of transport properties has a percolation character and is associated with loss of liquid-phase connectivity as the ice fraction grows.
- An analytical expression for the relative soil moisture diffusion coefficient has been derived, linking the hydraulic properties of the soil to its thermophysical characteristics and introducing a dimensionless parameter that determines the regime of moisture transport suppression during freezing.

The practical significance of the results lies in the fact that the proposed analytical expression represents a compact reduced model allowing description of moisture transport suppression in freezing soils without the need to solve the full coupled thermo-hydrological system. This enables its direct use as a physically based parameterization in regional and global land surface models (CLM, JSBACH, CryoGrid), models of seasonal and permafrost dynamics, engineering calculations of soil foundation stability, and prediction of the hydrological response of the cryosphere to contemporary climate change. The obtained results contribute to the theory of heat and mass transfer in freezing porous media and provide a basis for further development of numerical modeling methods for soil freezing processes.

References

1. Philip, J.R. The theory of infiltration: 1. The infiltration equation and its solution. *Soil Science*, 1957, vol. 83, no. 5, pp. 345–357. DOI 10.1097/00010694-195705000-00005
2. Šimůnek, J., van Genuchten, M.Th., Šejna, M. Development and Applications of the HYDRUS and STANMOD Software Packages and Related Codes. *Vadose Zone Journal*, 2008, vol. 7, no. 2, pp. 587–600. DOI 10.2136/vzj2007.0077
3. Lundin, L.-C. Hydraulic properties in an operational model of frozen soil. *Journal of Hydrology*, 1990, vol. 118, no. 1–4, pp. 289–310. DOI 10.1016/0022-1694(90)90264-X

4. Richards, L.A. Capillary conduction of liquids through porous mediums. *Physics*, 1931, vol. 1, no. 5, pp. 318–333. DOI 10.1063/1.1745010
5. Hansson, K., Šimůnek, J., Mizoguchi, M., Lundin, L.-C., van Genuchten, M.Th. Water flow and heat transport in frozen soil: numerical solution and freeze–thaw applications. *Vadose Zone Journal*, 2004, vol. 3, no. 2, pp. 693–704. DOI 10.2136/vzj2004.0693
6. Koopmans, R.W.R., Miller, R.D. Soil freezing and soil water characteristic curves. *Soil Science Society of America Proceedings*, 1966, vol. 30, no. 6, pp. 680–685. DOI 10.2136/sssaj1966.03615995003000060011x
7. Dall'Amico, M., Endrizzi, S., Gruber, S., Rigon, R. A robust and energy-conserving model of freezing variably-saturated soil. *The Cryosphere*, 2011, vol. 5, no. 2, pp. 469–484. DOI 10.5194/tc-5-469-2011
8. Darcy, H. *Les fontaines publiques de la ville de Dijon*. Paris: Victor Dalmont, 1856. 647 p.
9. van Genuchten, M.Th. A closed-form equation for predicting the hydraulic conductivity of unsaturated soils. *Soil Science Society of America Journal*, 1980, vol. 44, no. 5, pp. 892–898. DOI 10.2136/sssaj1980.03615995004400050002x
10. Mualem, Y. A new model for predicting the hydraulic conductivity of unsaturated porous media. *Water Resources Research*, 1976, vol. 12, no. 3, pp. 513–522. DOI 10.1029/WR012i003p00513
11. Spaans, E.J.A., Baker, J.M. The soil freezing characteristic: its measurement and similarity to the soil moisture characteristic. *Soil Science Society of America Journal*, 1996, vol. 60, no. 1, pp. 13–19. DOI 10.2136/sssaj1996.03615995006000010005x
12. Kozeny, J. Über kapillare Leitung des Wassers im Boden. *Sitzungsberichte der Akademie der Wissenschaften Wien*, 1927, Bd. 136, S. 271–306.
13. Carman, P.C. Fluid flow through granular beds. *Transactions of the Institution of Chemical Engineers*, 1937, vol. 15, pp. 150–166.
14. de Vries, D.A. Simultaneous transfer of heat and moisture in porous media. *Transactions of the American Geophysical Union*, 1958, vol. 39, no. 5, pp. 909–916. DOI 10.1029/TR039i005p00909
15. Cass, A., Campbell, G.S., Jones, T.L. Enhancement of thermal water vapor diffusion in soil. *Soil Science Society of America Journal*, 1984, vol. 48, no. 1, pp. 25–32. DOI 10.2136/sssaj1984.03615995004800010005x
16. Massman, W.J. A review of the molecular diffusivities of H_2O, CO_2, CH_4, CO, O_3, SO_2, NH_3, N_2O, NO, and NO_2 in air, O_2 and N_2 near STP. *Atmospheric Environment*, 1998, vol. 32, no. 6, pp. 1111–1127. DOI 10.1016/S1352-2310(97)00391-9
17. Celia, M.A., Bouloutas, E.T., Zarba, R.L. A general mass-conservative numerical solution for the unsaturated flow equation. *Water Resources Research*, 1990, vol. 26, no. 7, pp. 1483–1496. DOI 10.1029/WR026i007p01483
18. Zha, Y., Yang, J., Yin, L., Zhang, Y., Zeng, W., Shi, L. A modified Picard iteration scheme for overcoming numerical difficulties of simulating infiltration into dry soil. *Journal of Hydrology*, 2017, vol. 551, pp. 56–69. DOI 10.1016/j.jhydrol.2017.05.053

19. Carslaw, H.S., Jaeger, J.C. *Conduction of Heat in Solids*, 2nd ed. Oxford: Oxford University Press, 1959. 510 p.

20. Zhang, T., Frauenfeld, O.W. Soil Temperature and Active/Permafrost Layer Data over Global Land Areas. Boulder: NSIDC, 2011. Dataset G02189. DOI 10.7265/N5ZG6QF0

21. Oleson, K.W., Lawrence, D.M., Bonan, G.B. et al. Technical Description of Version 4.5 of the Community Land Model (CLM). NCAR Technical Note NCAR/TN-503+STR. Boulder: NCAR, 2013. DOI 10.5065/D6RR1W7M

22. Westermann, S., Schuler, T.V., Gisnås, K., Etzelmüller, B. Transient thermal modeling of permafrost conditions in Southern Norway. *The Cryosphere*, 2013, vol. 7, no. 2, pp. 719–739. DOI 10.5194/tc-7-719-2013

23. Ekici, A., Beer, C., Hagemann, S., Boike, J., Langer, M., Hauck, C. Simulating high-latitude permafrost regions by the JSBACH terrestrial ecosystem model. *Geoscientific Model Development*, 2014, vol. 7, no. 2, pp. 631–647. DOI 10.5194/gmd-7-631-2014